Pressure-induced amorphization and a possible polyamorphism transition in nanosized TiO_2: An x-ray absorption spectroscopy study

A.-M. Flank,[1,*] P. Lagarde,[1] J.-P. Itié,[1] A. Polian,[2] and G. R. Hearne[3]
[1]*SOLEIL Synchrotron, L'Orme des Merisiers, BP 48, F-91192 GIF/Yvette, France*
[2]*Physique des Milieux Denses, IMPMC, CNRS, Université Pierre et Marie Curie-Paris 6, 140 rue de Lourmel, 75015 Paris, France*
[3]*School of Physics & DST-NRF CoE in Strong Materials, University of the Witwatersrand, Johannesburg, South Africa*
(Received 20 March 2008; revised manuscript received 12 May 2008; published 25 June 2008)

The phenomenon of grain-size dependent pressure-induced amorphization (PIA) in TiO_2 nanomaterials has been evidenced by several experiments in recent years. This has stemmed mainly from x-ray diffraction (XRD) and Raman studies of ultrafine grained anatase. Until now there is no experimental evidence of the length scale of disorder nor is there a clear picture of the amorphous structures, specifically in the case of pressure amorphised anatase-TiO_2 starting material. The unresolved issues of the structural details and atomic-scale picture of the high-density amorphous (HDA) phase have now been addressed in an x-ray absorption spectroscopy (XAS) pressure study at the Ti *K*-edge. The local environment of the cation, to within a few nearest-neighbor shells, has been monitored up to ~30 GPa where the HDA phase is stabilized. In this phase the titanium atom is surrounded by 3 ± 0.5 oxygens at 1.89 Å and 3 ± 0.5 oxygens at 2.07 Å. The XAS results of this study suggest that a precursor ordered structural phase, different to that of anatase, is prevalent before amorphization occurs. The nature of this high-pressure stabilized precursor to amorphization likely depends on the starting experimental conditions at ambient pressure. In some cases this precursor has been identified as the columbite (α-PbO_2-type) crystalline structure perhaps with only limited range order. Samples of this type appear to evidence a "memory effect" in that after cycling into the HDA phase (up to 30 GPa) where complete structural disorder prevails, this α-PbO_2 structural intermediate is reestablished in a limited pressure range of the decompression cycle. It is also found that a new structure is stabilized in all cases of samples decompressed from the HDA phase to ambient conditions, characterized by fivefold coordinated Ti (2 ± 0.5 oxygens at 1.84 Å and 2.5 ± 0.5 oxygens at 2.06 Å) and is therefore structurally distinguishable from the HDA phase. These conceptual pictures are derived from the pressure dependence of both the extended x-ray-absorption fine structure (EXAFS) and the preedge parts of the absorption spectra.

DOI: 10.1103/PhysRevB.77.224112 PACS number(s): 61.05.cj, 64.70.Nd, 62.50.−p, 64.70.K−

I. INTRODUCTION

As is evident throughout the literature in recent years there is considerable interest in the physical properties of nanomaterials (in comparison to bulk analogs) and more specifically in the case of nano-TiO_2, due to both the intrinsic properties of the titanium oxide compound itself, and the modifications obtained because of the nanocrystalline character. Titanium oxide can be found in a number of crystallographic phases, some of which are stabilized only under high pressure or recovered by decompression to atmospheric pressure. The increase in surface to bulk ratio when the grain size reaches the nanoscale generally induces new physical properties, including unusual pressure responses.[1,2]

The behavior of single crystals of titanium dioxide rutile (tetragonal $I4_1/amd$) and anatase (tetragonal $P4/mnm$) under pressure at room temperature is well known.[3–6] During compression at ambient temperature anatase transforms first to a compound isostructural to columbite (orthorhombic α-PbO_2 type—Pbcn) at a pressure in the range 2–5 GPa, and then to a polymorph isostructural to the baddeleyite structure (monoclinic ZrO_2−$P2_1/c$) at $P > 10$ GPa. The transition pressures to new polymorphs seem to depend on the nature of the starting material, i.e., grain size, single- or polycrystalline state, defect and off-stoichiometry considerations and presumably the degree of hydrostaticity attained through the pressure medium used. The rutile form directly undergoes a pressure-induced conversion to a baddeleyite (monoclinic—$P2_1/c$) type structure, the onset pressure of which is at $P \sim 12$ GPa. Upon decompression of the bulk material to ambient conditions, the formation of an α-PbO_2-type structure is observed for both starting anatase and rutile polymorphs.

Surprisingly enough on the nanoscale (i.e., grain sizes of critical dimensions $d \sim 10$ nm or less), there is evidence that the starting anatase material is stable to higher pressure than in the bulk analog and pressure-induced amorphization (PIA) occurs at around 20 GPa. The pressure evolution of structural phases of nanoanatase starting material appears to be quite sensitively dependent on the average grain size. For instance, Swamy *et al.*[7] gathering different results obtained mostly by Raman spectroscopy and x-ray diffraction, describe a kind of phase diagram for these materials where, below a size of about 12 nm, there is a direct PIA pathway. In the range 12–40 nm anatase transforms into the baddeleyite-type structure and for grain sizes greater than $d \sim 50$ nm, the transition pathway often follows the anatase → α-PbO_2-type → baddeleyite sequence typical of the bulk. For nanoanatase below critical dimensions of $d \sim 4$ nm some degree of pressure-induced disorder has been predicted[1] by molecular dynamics simulations.

This paper presents an x-ray absorption spectroscopy (XAS) study of the pressure response of nanoanatase, of average grain size of ~6 nm, up to pressures of ~30 GPa at

room temperature. XAS, through the analysis of the fine structure in the extended regime (EXAFS) and of the pre-edge features, permits quite a detailed description of the local structure around a given atom, in this case the titanium, to be obtained. Therefore it is a well-suited technique to follow the evolution with pressure of the local environment, in particular when amorphization occurs.

II. EXPERIMENT

Samples of nanoanatase TiO_2 with an average grain size of 6 nm were synthesized from $TiCl_4$ by the hydrothermal method,[8] and characterization of the nanoanatase starting material was made by using both transmission electron microscopy (TEM) and x-ray diffraction. The Scherrer formula has been used to estimate an average particle size of diameter $d \sim 6$ nm from the (101) and (200) diffraction linewidths. The high-pressure XAS has been realized by means of a special diamond anvil cell (DAC), analogous to that described previously for perovskite studies.[9] The total thickness of the diamond anvils in the path of the incident beam has been reduced to 1 mm by using the perforated diamond-anvils concept to allow transmission experiments at the titanium *K*-edge (~ 5 keV). The anvils culet had a diameter of 200 μm, and the sample cavity drilled in an inconel gasket was about 80 μm in diameter. The pressure transmitting medium was silicone oil. Pressures above 30 GPa can be reliably attained with this assembly, and the pressure is measured through the fluorescence of a small ruby chip introduced near the sample. Coarse grained samples ($d \gg 50$ nm), representative of both bulk anatase and rutile, have also been investigated under very similar conditions in the same DAC, so as to represent reference systems. XAS experiments have been performed at the LUCIA beamline located at the Swiss Light Source.[10] This beamline delivers a high photon flux (around 10^{11} ph/sec) on a 3×3 μm^2 spot half-width at half maximum (HWHM) at the energy of the titanium *K*-edge. The incoming flux is monitored by the total electron yield signal from a 5 μm plastic foil covered by 800 Å of nickel, while the transmitted signal is measured by means of a silicon diode. At each pressure, three scans are added to increase the signal-to-noise ratio, leading to an overall recording time of 40 min per pressure step. Two Si(111) crystals were used as a monochromator and provide an energy resolution of 0.7 eV at the Ti *K*-edge. The energy calibration of the monochromator has been obtained by setting the first inflexion point of the absorption spectrum of a pure titanium foil to the value of 4966 eV. The scanned energy range is limited to 600 eV above the edge, due to the presence of Bragg peaks of the diamond anvils above this limit.

III. ANALYSIS AND RESULTS

A. Analysis methods

An XAS analysis starts with that of so-called model compounds (or references), for which the crystallographic data are well known. This ensures that the data acquisition and the extraction of the signal do not introduce spurious features. Here, the model compounds are the low-pressure bulk phases of rutile and anatase, the high-pressure baddeleyite phase and the α-PbO_2 structure obtained upon full decompression to ambient of the pressurized starting materials. All these experiments on microcrystals (grain sizes of several microns) have been conducted in the same DAC under very similar conditions used for the subsequent experiments on the nanophase samples.

The modeling of the EXAFS data has been done in a now classical way using the IFEFFIT package[11] which consists of a Victoreen modeling of the pre-edge region, a cubic spline modeling of the background after the edge and then a Fourier transform of the k^n-weighted residual $\chi(k)$ which gives the pseudo radial distribution function. All the experimental data have been processed using the same procedures and using the same set of parameters, so as to minimize random errors. To check this analysis, the data for the well-defined bulk compounds at ambient pressure have been modeled with the only free parameters being the Debye-Waller factors of the involved paths, since distances and coordination numbers are fixed by the crystallography. E_0 (absorption edge) and the so-called s_0^2 factor which describes the inelastic losses in the absorption process, were then kept fixed, independently of the pressure, and set at values determined from fitting the references. Figure 1 gives a comparison between the raw data for the two starting situations, namely the "macro-" and the nanoanatase samples at ambient pressure. Figure 2 shows the typical agreement which is obtained by the above analysis procedure for anatase after a full pressure cycle, i.e., the starting material converted to the α-PbO_2 form. The rest of the study of the nanoanatase will then mainly consist of comparisons between the different Fourier transforms, i.e., intercomparison of the nearest-neighbor shells of the pseudo radial distribution function.

The analysis of the pre-edge features located just below the main absorption edge consists, as already implemented by several other groups on different systems, of two steps. First a modeling of the background with a Lorentzian function which is then subtracted from the raw data and, second, a fitting of the overall structure by Voigt functions with a 50%–50% weighting of the Gaussian and Lorentzian parts. As is well documented now, there are three pre-edge peaks in the rutile structure that are usually labeled A1, A2, and A3. In anatase the second peak is split into two peaks, provided that the energy resolution is good enough. It may be noted that this splitting has also been observed and interpreted in rutile.[12,13] We have labeled these peaks in the case of anatase as follows: A1 ($\sim$4968.8 eV), $A'2$ ($\sim$4970.7 eV), A2 ($\sim$4972 eV), and A3 ($\sim$4974.5 eV) for the sake of consistency with rutile. The rutile pre-edge structure has been theoretically explained with different methods which mostly converge in their conclusions.[13,14] The first low-energy peak A1 is of purely quadrupolar origin (on-site Ti $1s \rightarrow 3dt_{2g}$) while its e_g counterpart is essentially superimposed on peak A2 and could be at the origin of peak $A'2$. A2 and A3 are of dipolar origin as a result of hybridization with orbitals from the second nearest-neighbor titanium atoms (t_{2g} and e_g parts of these 3*d* orbitals). The quadrupolar transitions are lowered in energy due to the core-hole effect. Finally the hybridization with nearest-neighbor oxygens, which occurs if there is an

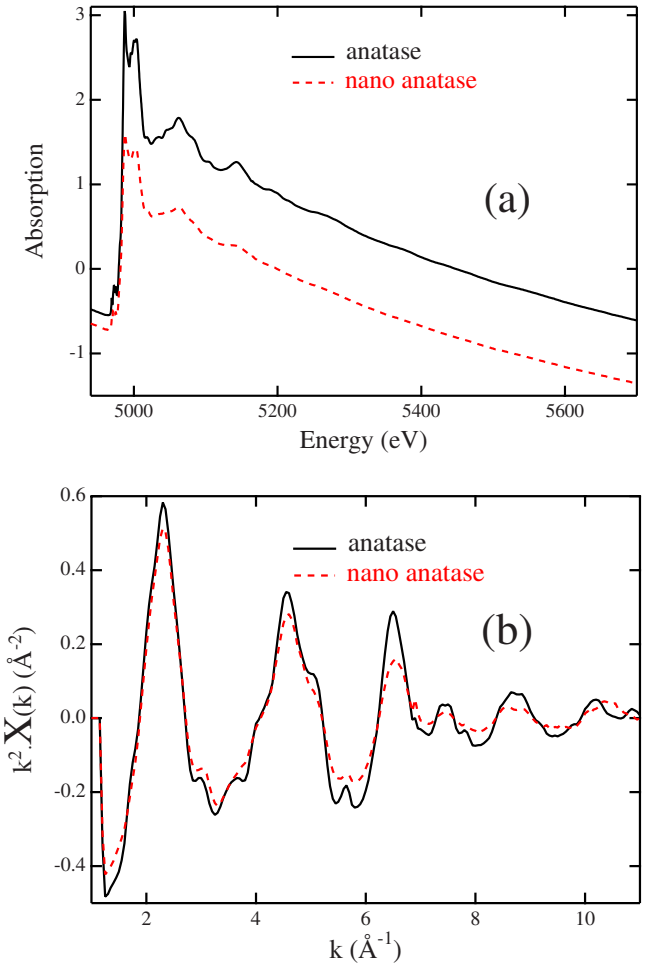

FIG. 1. (Color online) (a) Raw spectra for both bulk and nanoanatase samples at the Ti *K*-edge at ambient pressure measured in the diamond anvil cell. (b) Corresponding EXAFS signals.

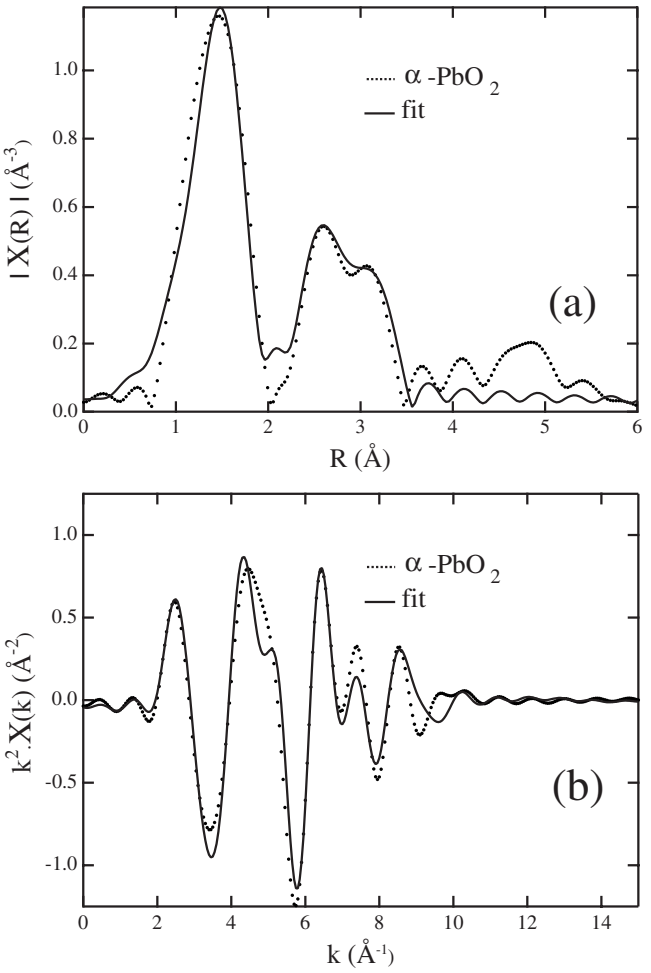

FIG. 2. Fit of the EXAFS data of bulk TiO_2 anatase transformed into the α-PbO_2 form after a full compression-decompression cycle (pressurized up to 21 GPa then decompressed to ambient). (a) shows the magnitude of the Fourier transform (FT) of the pseudo radial distribution function. (b) shows the k^2-weighted EXAFS. Only single scattering paths up to the seventh shell have been included.

absence of an inversion center (e.g., off-center character of the Ti atom in the octahedral environment of oxygens) as in the case of anatase, may also contribute to these peaks (mainly $A'2$).

B. Results

1. Bulk anatase and nanoanatase at ambient pressure

All experimental runs have been made with the same DAC in the same geometry. Figure 3 shows a comparison of the Fourier transforms of the EXAFS oscillations of bulk and nanoanatase at ambient pressure, both spectra collected inside the DAC. As expected they are very similar; the decrease in intensity of the peaks in the nanophase relative to those in the bulk is just a consequence of the size of the nanocrystals. Figure 3 also shows the pre-edge peaks for these samples. The intensity of the $A'2$ peak is much more intense for the nanophase sample than for bulk anatase. According to Farges *et al.*[15] this peak may be related to the amount of fivefold coordinated titanium, consistent with the increased amount of fivefold coordinated surface atoms in the nanocrystals.

2. Pressure-induced phase transition in nanocrystalline anatase

a. Extended x-ray-absorption fine structure data. Evidence for an amorphization transition. Four separate experiments have been done using the same sample batch and the same experimental conditions. These pressure sequences have been summarized in Table I. In all sets of data (series #1, #2, #3 and #4) the behavior up to 10 GPa appears to be identical, corresponding to a simple compression of the initial structure. Above this pressure some modifications in the spectra are observed. Results from series #2 differ from the results of the other series and will be discussed separately in this paper. The most detailed set of measurements also involving the highest resolution scans through the *K*-edge have been taken in series #3, and so the results of this series, representative of the behavior in series #1 and # 4 as well, will be discussed.

Figure 4 shows the evolution of the x-ray absorption near-edge spectrum (XANES) up to 20 GPa in series #3. The XAS spectra have first been carefully normalized in order to

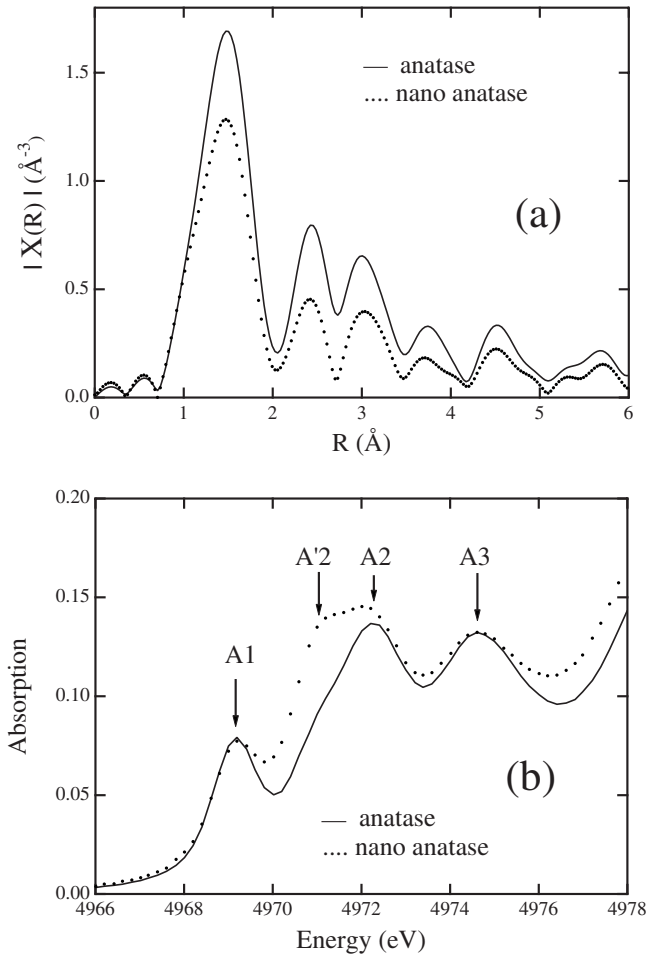

FIG. 3. (a) Comparison of the FT magnitude of the EXAFS of bulk and nanoanatase at ambient pressure; (b) shows the corresponding pre-edge part of the spectra.

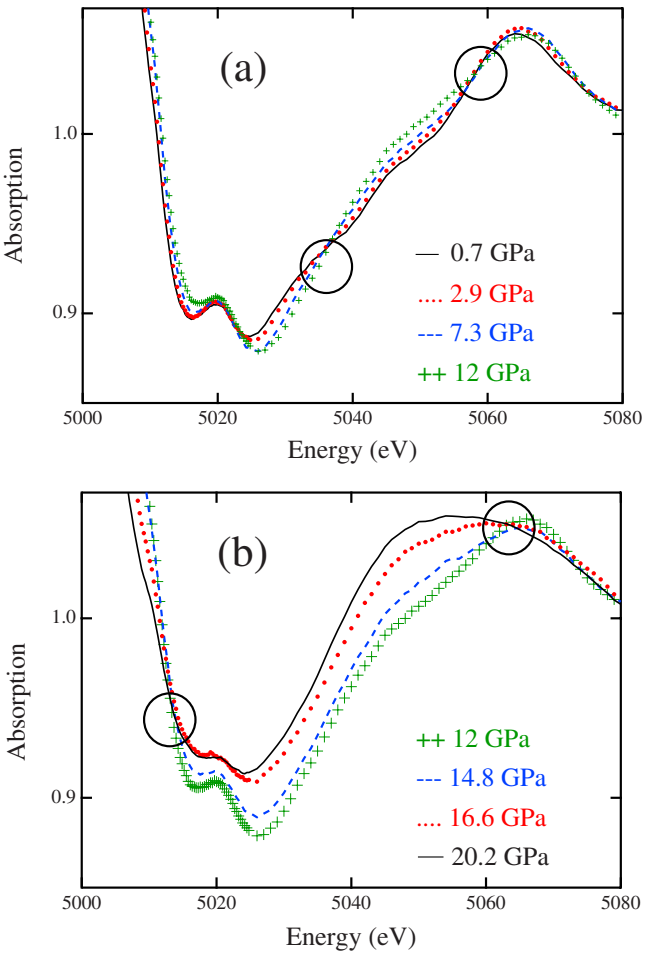

FIG. 4. (Color online) Evolution of the XANES spectra with increasing pressure from 0 to 12 GPa (a) and from 12 to 20 GPa (b) for the measurements of series #3, showing the two sets of isobestic points.

take into account the change in the overall absorption at high-pressure conditions. Isobestic ("stationary") points appear clearly, but at different energies below 15 GPa and above 15 GPa. The presence of isobestic points signifies that the sample has undergone a distinct structural phase change at some characteristic pressure in each of the pressures ranges indicated in Fig. 4. These are anatase→unidentified intermediate in the vicinity of 12 GPa and unidentified intermediate→high pressure amorphous structure onset at pressures above 15 GPa. The Fourier transforms of the EXAFS oscillations (Fig. 5) also show a difference in the pressure evolution in these two pressure ranges to corroborate the conclusion derived from the XANES evolutions depicted in Fig. 4. There is some degree of structural disruption of the anatase already occurring between 10 and 15 GPa to some (unidentified) intermediate-range crystallinity distinct from the anatase structure, and this is a precursor to amorphiza-

TABLE I. Sequence of pressure measurements for the four series of experiments on TiO_2 nanoanatase

	Compression	Decompression		
Series 1	0.3, 2.3, 5.5, 7.5, 9.8, 12.8, 15 and 16 GPa	4.7 GPa and ambient pressure		
Series 2	0.3, 10.8, 15.7, 20, 25 and 31 GPa	11, 6.3 GPa and ambient pressure		
Series 3	1, 1.9, 2.9, 4, 7, 10, 12, 14.5, 16.7, 20 GPa	17.8, 15.9, 14, 12, 10.5, 8.8, 7, 4.7, 2.6, 1.5 GPa and ambient pressure		
Series 4	0.5 to 15 GPa	3.5 GPa	Recompression 3.5→21 GPa	Decompression 21 GPa→ambient

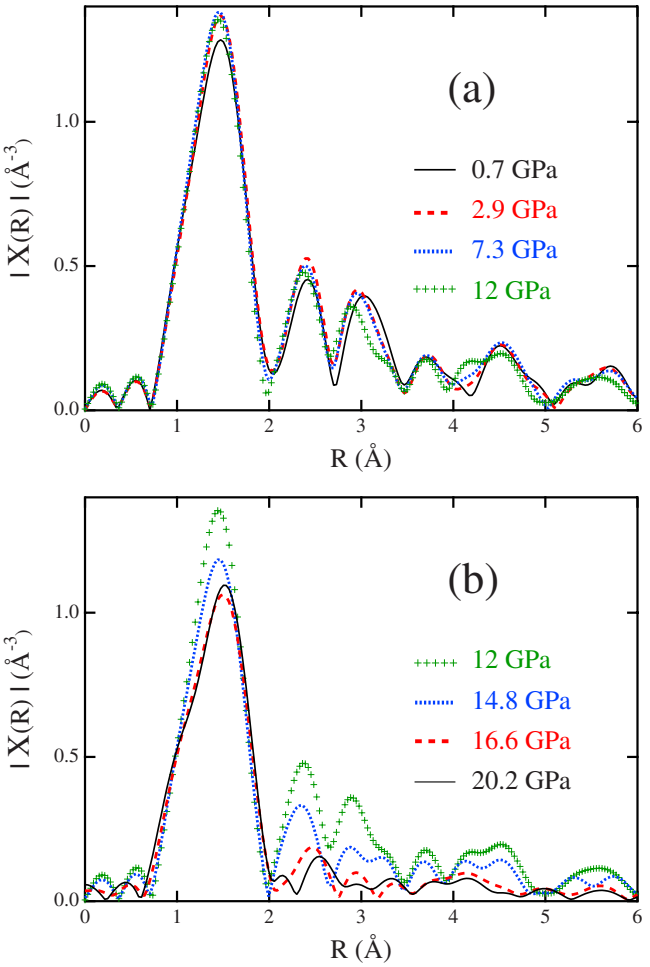

FIG. 5. (Color online) The magnitudes of the Fourier transforms corresponding to experiments in series #3 of Fig. 4. Note in panel (a) at 3.3 and 4.2 Å in the 12 GPa spectrum the signatures of the structural intermediate that emerges prior to amorphization.

tion. The previous Raman and x-ray diffraction (XRD) pressure studies of Pischedda *et al.*[1] would then suggest that the original anatase phase coexists with this new intermediate-range crystalline phase. Complete disorder becomes evident above 15 GPa where coordination shell signatures beyond the oxygen nearest-neighbor distances show an appreciable reduction in intensity.

Moreover, in series #4, pressure has been increased only to 15 GPa and then decreased to 3.5 GPa. Figure 6 shows that the XANES spectra of series #4 (0 GPa), series #3 (0 and 4 GPa upstroke) are identical, with only a very slight effect of the pressure, but the XANES of the 3.5 GPa downstroke of the sample in series #4 is definitely different. This emphasizes that the compression to 15 GPa (prior to amorphization) modifies the structure of the anatase sample to that of a new phase at least involving mid-range order over several coordination shells, and this modification is not reversible.

In all series the amorphization begins in the 15–20 GPa pressure range and discerned up to 30 GPa, the highest pressure of this study. This is evidenced by the lack of any peak structure in the pseudo radial distribution function beyond

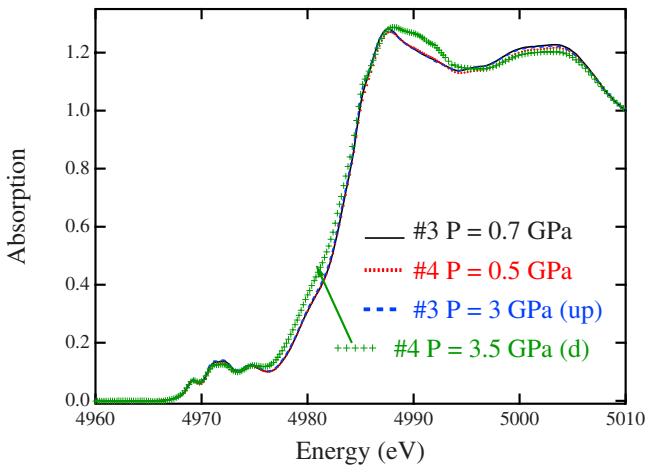

FIG. 6. (Color online) XANES part of the absorption spectra of nanoanatase for series #3 and #4, at near ambient pressure and in the vicinity of 3 GPa upstroke (up) and downstroke (d). Downstroke spectrum shows the irreversibility after the sample in series #4 has been compressed to the highest pressure of 15 GPa (see text).

2 Å (Fig. 7). This suggests progressive collapse of an ordered network on a scale of ~2 Å and beyond, i.e., extending beyond the first nearest-neighbor shell. The first shell, attributed to the nearest-neighbor oxygen environment, exhibits a structure which may be deduced from the unresolved splitting of this shell into two groups of interatomic distances. Values of 3 ± 0.5 at 1.89 Å and 3 ± 0.5 at 2.07 Å have been derived from the fitting procedure in the EXAFS analysis.[11] It appears that the average Ti-O distance is larger in the high-pressure amorphous phase than in the lower-pressure phases (with an octahedral environment around the Ti atom). This is generally observed with an increase in the coordination number. Such a behavior is expected for a transition to the baddeleyite phase, where the oxygen coordination increases from 6 to 7. In the case of the amorphous high-pressure phase, the oxygen polyhedron is strongly dis-

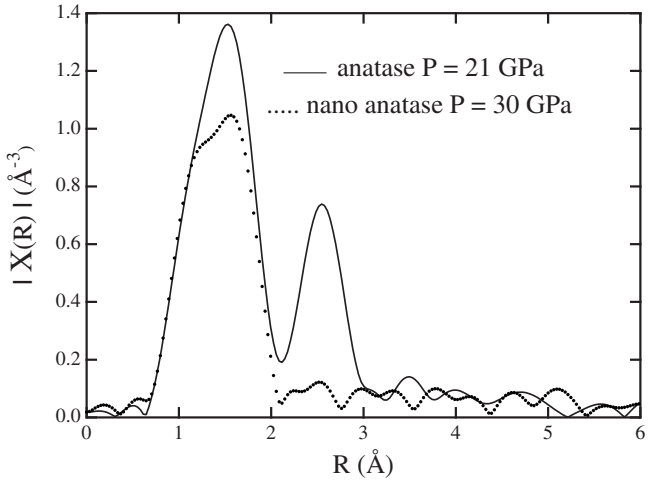

FIG. 7. FT Magnitude of EXAFS of the HDA form of nanoanatase measured at 30 GPa, compared to the high-pressure form of bulk TiO_2 at 21 GPa (i.e., baddeleyite-type phase).

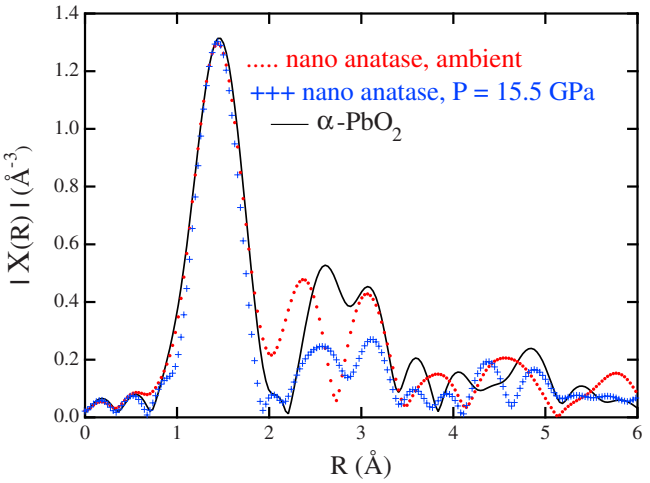

FIG. 8. (Color online) Comparison of FT magnitude of nanoanatase (series # 2) at ambient pressure (red), compressed up to 15 GPa (crosses, blue) and bulk anatase decompressed to ambient pressure after pressurizing to 21 GPa, to obtain the α-PbO_2 form of TiO_2 (black). Note the similarity in peak features (positions) of the phases obtained at 15 GPa upon compression, and that of the α-PbO_2 form of TiO_2.

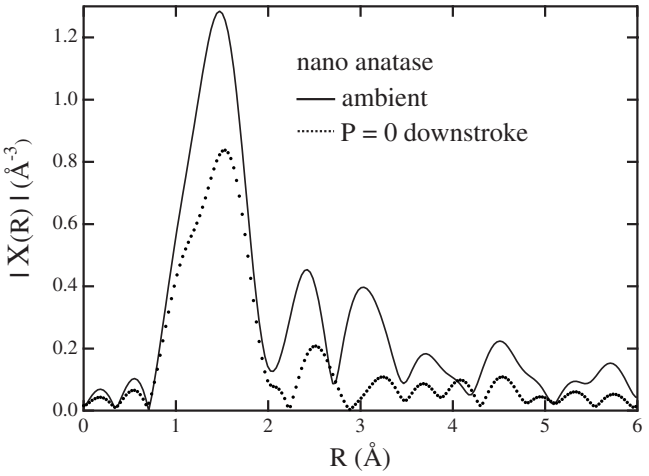

FIG. 9. Comparison between the Fourier transforms of pristine nanoanatase (series #3) at ambient pressure and that observed after a full compression-decompression cycle showing the decrease in the coordination number of the first oxygen shell.

torted and cannot be fitted using a local environment similar to that of the baddeleyite phase. The EXAFS analysis provides the experimentally deduced atomic-scale picture of the high-density amorphous (HDA) phase of nano-TiO_2. This is information which cannot be derived from the previous XRD and Raman pressure data dominated by a broad featureless spectral envelope typical of a highly disordered phase.

Transition through an α-PbO_2 *phase pathway (as exemplified by series #2).* The behavior in the vicinity of 15 GPa is more peculiar for the series #2. At this pressure, the change of the local structure does not correspond to a progressive destruction of the long-range order prior to an amorphization. Instead the Fourier transform becomes very similar to that of the decompression product found when the bulk anatase has been compressed to 21 GPa and then relaxed down to atmospheric pressure (see Fig. 8), i.e., the α-PbO_2 form of TiO_2 obtained after such a pressure cycle.

For nanoanatase of an average grain below a critical value $d \sim 10$ nm, there seems up to now to be a consensus (based on XRD and Raman pressure data) that there is only a direct transition from nanoanatase to a disordered phase, whose onset is at ~ 20 GPa. The transition to other lower-symmetry crystalline forms (either α-PbO_2 or baddeleyite at transition pressures of ~ 5 and ~ 12 GPa, respectively) has only been observed for larger grain sizes, and the transition pressures are somewhat dependent on various extrinsic factors.

We have presented evidence here that, for the nanophase sample with an average grain size of 6 nm, a transition to crystalline phases with intermediate-range structure does occur, preceding the PIA.

Upon decompression from the highest pressure of 30 GPa in the series #2, a singular point appears again at ~ 11 GPa where both, (*i*) the first oxygen shell narrows and retrieves almost the shape it had at the first structural transition to α-PbO_2-type during the pressurization similar to that depicted in Fig. 8 and (*ii*) a peak at long distances is again present, around 2.5 Å, very close to that found in α-PbO_2 with a decrease in the intensity of the second component at 3 Å. Therefore, from a local point of view around the titanium atoms, it seems that a kind of recrystallization to a phase very similar to α-PbO_2 takes place when the pressure is relaxed from 30 GPa down to 11 GPa, although true medium- to long-range order is not very well defined. Moreover it appears that this structural situation is transient, in that upon further decompression to ~ 6.5 GPa and lower, the system stabilizes into a disordered structure once again with a distorted first shell, and comparable to the final (recovered) product obtained in the other series of experiments.

Return to ambient pressure. In all series of measurements the final step down to atmospheric pressure induces a new local structural transition: The first shell undergoes a definite drop in intensity and it appears now composed of an asymmetric peak, which can be fitted by two subshells of 2 ± 0.5 O at 1.84 Å and 2.5 ± 0.5 O at 2.06 Å, suggesting an overall fivefold coordination (Fig. 9). The Fourier transform does not exhibit any defined structure beyond the first shell, except a very slight contribution at the distance of the second peak observed in baddeleyite or α-PbO_2, which means that this structure is very poorly crystallized. However, it appears difficult to give a detailed structural description of this kind of "low-density amorphous" (LDA) end product except perhaps to assert that it is definitely quite distinct from the HDA phase.

b. Pre-edge structure. The pre-edge structures for the various structural forms of TiO_2 at ambient pressure are different and therefore they are very sensitive to the modification of short- and long-range orders. For Ti atoms in an octahedral environment of oxygen (distorted or not), the origin of the different contributions to these structures is well documented and has been described in the introduction.

This description, valid only for an octahedral environment, is mainly related to the crystal-field splitting of the titanium 3*d* orbitals and therefore is not applicable for an-

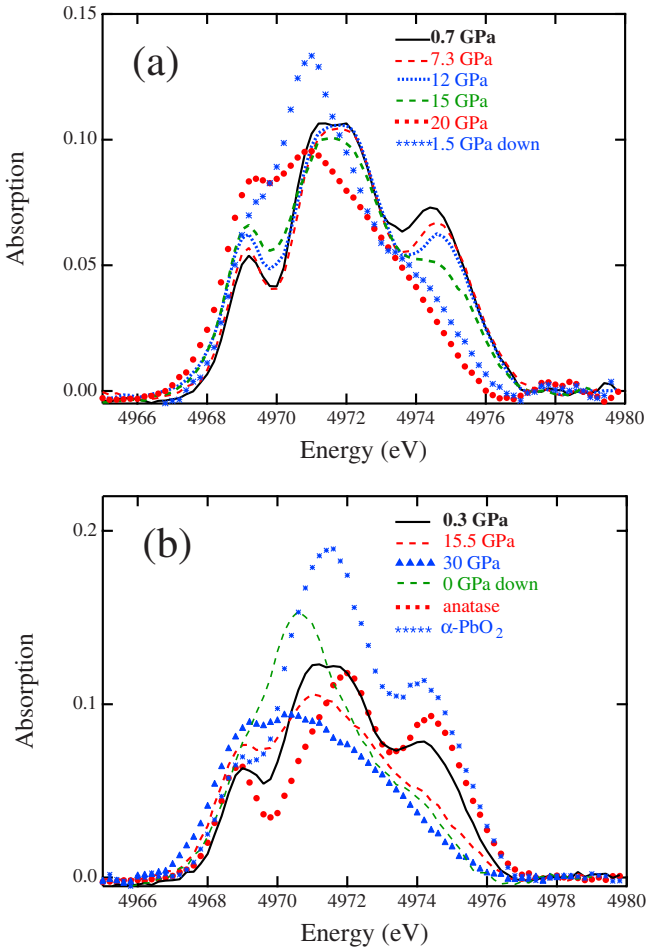

FIG. 10. (Color online) Evolution of the pre-edge peaks of nano-TiO_2, (a) series #3 and (b) series #2.

other type of local environment. For example in a tetrahedral environment the origin of the pre-edge, which is more intense in this geometry, would be clearly different. In the case of the high-pressure phase of TiO_2 (baddeleyite), to the best of our knowledge, no calculation of the pre-edge part has been performed. Nevertheless, the shape of the pre-edge constitutes a fingerprint of the structure. Therefore it is considered interesting to follow the pressure evolution of the pre-edge structure in order to elucidate the phase transformation sequence of the pressurized nano-TiO_2.

Figure 10(a) shows the pre-edge part of the absorption spectra obtained at different pressures for various phases of series #3. As already pointed out, the nature of the structural phase evolution with pressure is somewhat different for the series #2, therefore we will discuss the results obtained in each of these series independently.

In all series the spectra obtained up to 12.2 GPa are similar to that taken at ambient pressure, except for a minor change in the intensity and in the position of the A3 peak. The overall shape remains similar, which indicates only a small variation in the structure: The Ti is still in an octahedral configuration, confirming the results of the EXAFS analysis. At higher pressure, around 15 GPa, a pronounced modification of the pre-edge spectrum occurs. Here again we have a good agreement with the EXAFS analysis. At 30 GPa, the shapes of the four peaks have definitely changed, the most evident signature being the sudden intensity drop of the peaks $A'2$, A2, and A3. The intensity decrease of these peaks, which are theoretically explained by the hybridization of the central Ti $3d$-orbitals with those cations from the neighboring octahedra, is consistent with a picture of amorphization of the structure. When the pressure is fully released, a new spectrum is observed with the appearance of a very intense peak close to 4971 eV. This spectrum may be compared with the one observed for nanocrystalline sol-gel anatase samples,[16] where the intense peak was attributed to a reduced coordination of Ti atoms, mainly in fivefold coordination.[15] This is supposed to signify a totally different structure of the material in the recovered specimen which may be referred to as the LDA phase, as opposed to the HDA phase stabilized above 15 GPa. Here again there is a good agreement with the EXAFS results.

In series #2 both HDA and LDA spectra are identical to the spectra obtained in the other series [Fig. 10(b)]. The main difference in this series is the EXAFS spectrum obtained at 15.5 GPa. At this pressure the EXAFS analysis indicates that the sample is partly in an α-PbO_2 structure although the pre-edge spectrum does not match that of the α-PbO_2 decompression product obtained from bulk TiO_2. A strong decrease of the A3 peak is again observed, as in the case of the HDA phase. An explanation then is that the sample is not pure α-PbO_2 and coexists with the emergent HDA phase. This is not necessarily contradicted by the EXAFS data, which evidence mostly the ordered part of the sample. Therefore at $\sim$15 GPa in this series the structure observed in the Fourier transform of the EXAFS oscillation above 2 Å reflects only the contribution of the α-PbO_2 phase.

IV. CONCLUSIONS

There is always a problem of definition of the disorder in solid materials, and how it is possible to discriminate between glassy, amorphous, and poorly crystallized samples. The existence of a glass transition temperature measured from the viscosity is a clear signature of the glassy state. The difference between purely amorphous and poorly crystallized samples is more difficult to define. Here, by means of a technique very sensitive to the kind of local order around one given atom, namely the titanium, there is evidence that nanoanatase of an average grain size $\sim$6 nm, exhibits in all cases a pressure driven disorder on a scale of $\sim$2 Å. This is supposed to be indicative of a purely amorphous network, i.e., with a disorder beyond the first nearest-neighbor shell. This amorphization whose onset lies in the 15–20 GPa range is evident in either the EXAFS or through the behavior of the titanium pre-edge peaks. The full release of pressure to ambient conditions results in a LDA compound. This is different from the recovered product of bulk anatase starting material after a full compression-decompression cycle. It is also different from the HDA phase, i.e., TiO_2 is one more example where polyamorphism takes place. In all experiments starting from the same batch of nanoanatase, there is a transition

of crystalline anatase to an intermediate-range crystalline phase prior to amorphization with an onset at pressures above ~15 GPa. In one series, the α-PbO_2-type structure has been detected at ~15 GPa together with a partial amorphization. In this last case, the decrease in pressure from the HDA phase regime proceeds first via a recrystallization pathway to a α-PbO_2-type structure (discerned at ~11 GPa). This suggests that there is a kind of memory effect of the compression pathway, before reverting to a LDA phase similar to what is seen in the other series suite of experiments upon decompression to ambient conditions.

Considerations that arise from these results, and that have not been addressed in the previous (Raman and XRD) investigations of this size dependent PIA, are as follows:

(i) There may be very different structural pathways which evolve at pressure although they originate from the same batch of ultrafine grained nanomaterial. The "phase diagram" as exemplified by this case of nanoanatase starting material as a function of pressure is not uniquely defined, and the evolution of the sample appears to be sensitively dependent on the "pressure conditions." To rationalize this we propose that there may be some pressure influenced sintering (grain-growth) phenomenon between different particles of an appropriate orientation, so that the sample behaves locally as if it was made of larger grain-size particles ($d > 50$ nm). This means that the ultrafine grain-size identity ($d < 10$ nm) is lost. Actually, this behavior has also been invoked to explain recent results obtained by x-ray diffraction upon a P-T treatment.[17] Alternatively the batch of ultrafine grained starting nanoanatase material is such that there are possible nucleation sites for the emergence of the α-PbO_2-type intermediate as it is the case for the bulk material. The polymorph (α-PbO_2-type) intermediate occurs at pressures before the end-point transition to the energetically favored HDA (at P ~20 GPa). This is perhaps a corroboration of the idea that there is an extreme sensitivity of the P-T phase diagram to grain-size identity in the case of nano-TiO_2, and perhaps in many other nanostructured systems as well. Whatever the structural transition route, the behavior is very distinct from that of the bulk since the HDA phase and not the baddeleyite phase is stabilized at pressures above 20 GPa. It may be noted that for the microanatase of this work, considered here as bulk reference material, we observe that the first transition to α-PbO_2-type and baddeleyite occurs at higher pressures (~12 GPa and ~18 GPa, respectively) than previously reported. It has already been indicated in the introduction that there are various factors that influence these transition pressures in the bulk.[3,17]

(ii) For all sets of experiments on nano-TiO_2 completed in this work, the recovered amorphized end product is a new structural phase, highly disordered as is the HDA phase but comprising fivefold coordinated titanium motifs. This LDA decompression product is radically different to what is obtained after the same cyclic pressure sequence has been applied to either bulk rutile or anatase starting materials.

(iii) In previous studies the set of pre-edge peaks has been widely used as a signature of the local symmetry around the titanium atom, either from theoretical considerations or empirical observations. It is advisable, as evidenced in this study, that the behavior of these peaks be considered in conjunction with the results from the local structure (EXAFS) analysis. The summary interpretation of the pressure behavior of the pre-edge features is as follows:

(a) Above 20 GPa, the amorphization process induces a strong modification of the pre-edge peaks corresponding to a change in the local environment around the Ti atom (loss of medium-range order, loss of octahedral configuration, and increase in the coordination number). Therefore, a simulation of the pre-edge part of the absorption spectrum will require new calculations based on a crystalline model energetically close to that of the HDA phase (for example, the baddeleyite structure).

(b) It may be noted that the contributions to the peak $A'2$ must have multiple origins, including both the interaction of Ti with neighboring oxygen atoms when there is no inversion center in the structure (off-center Ti in the octahedron as it is the case for bulk anatase) and the existence of fivefold coordinated Ti. Indeed the return to atmospheric pressure leads to a new structure which is suggested by the EXAFS analysis to be composed mainly of fivefold coordinated titanium (2 ± 0.5 O at 1.84 Å and 2.5 ± 0.5 O at 2.06 Å). At the same time we see a strong increase in both the A2 and $A'2$ peak intensities.

Finally, the use of combined experiments where Raman spectroscopy, XRD, and XAS are recorded at each pressure step would be of paramount importance for a full description of the behavior of such a system but, to the best of our knowledge, such a setup is still not available.

ACKNOWLEDGMENTS

This work was performed at the Swiss Light Source, Paul Scherrer Institut, Villigen, Switzerland. We are grateful to the machine and beamline groups whose outstanding efforts have made these experiments possible. G.R.H. acknowledges partial funding from a CNRS-NRF collaborative source (Grant No. UID 62105).

*To whom correspondence should be addressed; anne-marie.flank@synchrotron-soleil.fr

[1] V. Pischedda, G. R. Hearne, A. M. Dawe, and J. E. Lowther, Phys. Rev. Lett. **96**, 035509 (2006).

[2] G. R. Hearne, J. Zhao, A. M. Dawe, V. Pischedda, M. Maaza, M. K. Nieuwoudt, P. Kibasomba, O. Nemraoui, J. D. Comins, and M. J. Witcomb, Phys. Rev. B **70**, 134102 (2004).

[3] T. Arlt, M. Bermejo, M. A. Blanco, L. Gerward, J. Z. Jiang, J. S. Olsen, and J. M. Recio, Phys. Rev. B **61**, 14414 (2000).

[4] J. C. Jamieson and B. Olinger, Science **161**, 893 (1968).

[5] J. K. Dewhurst and J. E. Lowther, Phys. Rev. B **54**, R3673 (1996).

[6] H. Sato, S. Endo, M. Sugiyama, T. Kiewgawa, O. Shimomura, and K. Kusaba, Science **251**, 786 (1991).

[7] V. Swamy, A. Kuznetsov, L. S. Dubrovinsky, P. F. McMillan, V. B. Prakapenka, G. Shen, and B. C. Muddle, Phys. Rev. Lett. **96**, 135702 (2006); V. Swamy, A. Kuznetsov, L. S. Dubrovinsky, R. A. Caruso, D. G. Shchukin, and B. C. Muddle, Phys. Rev. B **71**, 184302 (2005); V. Swamy, L. S. Dubrovinsky, N. A. Dubrovinskaia, F. Langenhorst, A. S. Simionovici, M. Drakopoulos, V. Dmitriev, and H.-P. Weber, Solid State Commun. **134**, 541 (2005); V. Swamy, L. S. Dubrovinsky, N. A. Dubrovinskaia, A. S. Simionovici, M. Drakopoulos, V. Dmitriev, and H.-P. Weber, *ibid.* **125**, 111 (2003).

[8] H. Yin, Y. Wada, T. Kitamura, T. Sumida, Y. Hasegawa, and S. Yanagida, J. Mater. Chem. **12**, 378 (2002); P. Franklin, M.S. thesis, University of the Witwatersrand, 2004.

[9] J.-P. Itié, B. Couzinet, A. Polian, A.-M. Flank, and P. Lagarde, Europhys. Lett. **74**, 706 (2006).

[10] A.-M. Flank, G. Cauchon, P. Lagarde, S. Bac, M. Janousch, R. Wetter, J.-M. Dubuisson, M. Idir, F. Langlois, T. Moreno, and D. Vantelon, Nucl. Instrum. Methods Phys. Res. B **246**, 269 (2006).

[11] B. Ravel and M. Newville, J. Synchrotron Radiat. **12**, 537 (2005); J. J. Rehr and R. C. Albers, Rev. Mod. Phys. **72**, 621 (2000).

[12] J. C. Parlebas, M. A. Khan, T. Uozumi, K. Okada, and A. Kotani, J. Electron Spectrosc. Relat. Phenom. **71**, 117 (1995).

[13] P. LeFèvre, H. Magnan, D. Chandesris, J. Jupille, S. Bourgeois, W. Drube, H. Ogasawara, T. Uozumi, and A. Kotani, J. Electron Spectrosc. Relat. Phenom. **136**, 37 (2004).

[14] Y. Joly, D. Cabaret, H. Renevier, and C. R. Natoli, Phys. Rev. Lett. **82**, 2398 (1999).

[15] F. Farges, G. E. Brown, Jr., and J. J. Rehr, Phys. Rev. B **56**, 1809 (1997).

[16] V. Luca, S. Djajanti, and R. F. Howe, J. Phys. Chem. B **102**, 10650 (1998).

[17] Y. Wang, Y. Zhao, J. Zhang, H. Wu, L. Wang, S.-N. Luo, and L. L. Daemen, J. Phys.: Condens. Matter **20**, 125224 (2008).